buildings

IMPACT FACTOR 3.4

CITESCORE 5.6

Article

Uncovering Future Mold Risk in Existing Residential Walls with Climate Change

Pamela L. Cabrera, Kayla Baker and Holly Samuelson

Special Issue
Climate Resilient Buildings: 2nd Edition

Edited by
Dr. Michael A. Lacasse and Dr. Marzieh Riahinezhad

MDPI

https://doi.org/10.3390/buildings16132643

buildings

Article

Uncovering Future Mold Risk in Existing Residential Walls with Climate Change

Pamela L. Cabrera [1,2,†], Kayla Baker [3,4,†] and Holly Samuelson [4,5,*]

1 Transsolar Inc., New York, NY 10003, USA; pamela.cabrera@cooper.edu
2 The Irwin S. Chanin School of Architecture, Cooper Union, New York, NY 10003, USA
3 Aurora Energy Research, Sydney, NSW 2000, Australia
4 Faculty of Arts and Sciences, Harvard Graduate School of Design, Harvard University, Cambridge, MA 02138, USA
5 Department of Architecture, Massachusetts Institute of Technology, Cambridge, MA 02139, USA
* Correspondence: hollysam@mit.edu
† These authors contributed equally to this work.

Abstract

This paper examines the vulnerability of wood-framed residential building envelopes to mold growth under projected future climate conditions, specifically elevated temperatures and humidity, a topic that is rarely addressed in the climate resilience literature. Residential exterior walls designed with interior insulation and vapor-retarding membranes may prove inadequate in future conditions. This study combined hygrothermal simulation and mold growth computation using morphed future weather data to analyze archetypal walls from two construction eras (1990s–2000s and present) in three US cities: New York City, Philadelphia, and Washington, DC. The results show substantial increases in mold's prevalence under future climate scenarios for historical code-compliant walls, with even greater risk in walls with highly impermeable vapor barriers. Contemporary code-compliant walls showed no increased risk of mold. This framework for assessing future hygrothermal risks in building envelopes suggests a potentially widespread resilience problem. It underscores the need for further research, especially given the vast inventory of existing wood-frame buildings from earlier eras.

Keywords: mold risk; mould risk; hygrothermal simulation; climate resilience; housing; moisture; building envelope

1. Introduction

1.1. Climate Change and Housing Construction

Since 2001, the Intergovernmental Panel on Climate Change (IPCC) has urged cities to understand the need to adapt building codes to future climates [1]. Climate change alters long-term weather patterns, with the potential to drastically affect the built environment and the performance of the existing building stock. The research efforts thus far have focused on the impact on energy consumption [2,3] or on the impacts of sea-level rise, storm surge, and changes in rainfall [4,5]. Even though there is a growing number of studies in academic journals covering the hygrothermal sensitivity of wood envelope assemblies to higher temperatures and absolute moisture levels in future climates [6–10] and increased rain leakage or air tightness [11–13], none have studied the resulting mold growth risk on the existing US timber-framed homes in this highly populated area (Climate Zone 4A) and prevalent era of construction (homes built in accordance with building codes from the

Check for updates

Academic Editor: Antonio Caggiano

Received: 30 April 2026
Revised: 20 June 2026
Accepted: 25 June 2026
Published: 2 July 2026

1990s onwards). Research on the matter is urgent, especially in lightweight and layered building envelopes with moisture- and vapor-retarding membranes designed for historical climatic conditions.

In the United States (US), current building codes and practices are based on climate zones defined by ASHRAE (formerly known as the American Society of Heating, Refrigerating, and Air-Conditioning Engineers). Previous research shows that future conditions will shift these climate zones [14], and experts argue that we should anticipate future climates in current building codes [15], as this is a pressing matter that should be addressed urgently [16]. Existing buildings will be exposed to unprecedented changes in the upcoming years. Identifying emerging risks can help guide adaptation decisions to achieve greater climate resilience in buildings [17,18].

Our research focuses on ASHRAE Climate Zone 4A along the east coast of the US (Cfa humid subtropical in the Köppen climate classification system), characterized as mixed-humid [19]. The National Climate Assessment predicts that with a 2 °C global air temperature increase from pre-industrial levels, precipitation in ASHRAE Climate Zone 4A could increase the 1991–2020 baseline by 5% to 7%, and the magnitude of this change would increase to 10% to 15% under a 4 °C increase in global air temperature [20]. Due to these changes, we expect substantial shifts in the hygrothermal performance of exterior walls, affecting their moisture diffusion and moisture saturation. The two main factors for this shift in performance are the rise in the absolute moisture content in the air [21] and the greater temperature difference between the exterior and the mechanically cooled interior, with seasonal shifts that will prolong the cooling season.

In the US, residential exterior walls have typically incorporated layered lightweight wood-frame wall assemblies. For instance, 93% of single-family homes and 83% of multi-family buildings completed in 2018 were wood-framed [22]. In recent decades, these wall assemblies have included interior insulation to mitigate heat loss and moisture-control membranes to prevent condensation inside the wall assembly, especially in cold weather [23]. Such walls, and the building codes that govern their design, have been planned for a narrow range of historical exterior climates and may be ill-prepared to respond to changing exterior conditions. In the northeastern US, building codes have been designed around cold winters and relatively mild summers. Therefore, existing and newly constructed buildings in this region may not perform well in the warmer climates predicted for the future.

1.2. Moisture and Mold

Today, people spend most of their time indoors [24,25]; consequently, indoor environmental quality directly affects their health and well-being. Moisture control is a significant concern in building envelope design, as it can lead to mold growth and poor indoor environmental quality [24]. Mold emits a mix of particulates (e.g., spores) and volatile organic compounds, which have been shown to affect human health. The World Health Organization has linked indoor mold to an increased risk of allergies, asthma, respiratory problems, and immune reactions [26]. Research at the Lawrence Berkeley National Laboratory concluded that building dampness increases health risk effects by 50% [27]. Simultaneously, the presence of mold can entail non-health-related financial consequences, as it may indicate high moisture content in the materials, thereby reducing insulation's effectiveness and leading to rot in wood [28].

Most building materials contain sufficient nutrients to support mold growth [29], and lightweight timber building envelopes with interior insulation are particularly prone to it. In susceptible wood-based materials, mold begins to grow at a relative humidity threshold of 75–80% at temperatures above 5 °C (41 °F) [30], and the most critical factor for mold growth is moisture content [31]. Wood is a hygroscopic material and is affected quickly by the humidity of the air boundary layer at its surface. The wood species most commonly used for lightweight structural residential framing are pine and spruce sapwood, and both species show very high sensitivity to mold growth in laboratory studies by Viitanen [31].

1.3. Moisture and Mold Growth Modeling

The resilience of current façade designs to future climate-related stresses has been largely underexamined. While the hygrothermal performance and mold-inhibiting properties of building envelopes have been relatively well studied [18,32], the existing literature has rarely considered future weather conditions or a changing climate in mold growth simulations for testing building envelopes' performance [33], with notable exceptions such as Schroderus et al. [34], who included mold performance in the investigated impacts of building retrofits in Finland.

Understanding resilience to mold growth in a building envelope requires analyzing the temperature and moisture content of each material over time. This is more comprehensive than traditional hygrothermal studies focusing on vapor condensation within an envelope assembly. This analysis is possible with numerical modeling, such as with the software Wärme und Feuchte Instationär (WUFI), (WUFI 2D v4.5.0, Fraunhofer Institute for Building Physics, Holzkirchen, Germany) [35,36]. The validity of the WUFI 2D simulation has been tested against field measurements of moisture levels in building materials by several researchers [37,38]. The dynamics of biological activity and environmental conditions can yield non-intuitive outcomes [39]; simulation, therefore, provides a valuable tool for analyzing mold growth. Researchers are producing a growing body of literature on the risk of mold growth, and mathematical models have been developed for material categories in the building envelope based on temperature and moisture content [30,38,40].

While researchers have used such methods to study the risks of mold growth in future climates, the studies have been limited, for example, to geographies such as Canada and Northern Europe, and to historical brick facades [41], newly proposed façade systems [42], or rainwater wetting [43]. This study advances and expands the analysis by using 2D hygrothermal simulation to investigate prevalent new and historical wood-framed construction methods in the populous northeastern US under daily temperature and humidity conditions. This research aims to determine the potential for mold growth on historical and current code-compliant building facades when exposed to the humidity and air temperature levels expected over the building's design life. This research aims to fill a gap in the academic literature and determine the resilience of existing building facades to climate change.

2. Materials and Methods

2.1. Research Overview

This research examines long-term shifts in the seasonal patterns of humidity and temperature expected with climate change. Acute or shock events that may further exacerbate mold growth are disregarded. Therefore, we neglect water leaks caused by events such as increased rainfall intensity, storms, flooding, and sea level rise. Our strategy is conservative, providing a baseline understanding of potential mold growth in future climates. Specifically, we study the diffusion of moisture driven by temperature, air pressure, and vapor pressure differences across exterior walls, ultimately driven by differences between the indoor and outdoor climates. This research expands on an earlier study by the authorship team [44,45] by broadening the geographic scope to include two more cities, comparing two types of timber frame exterior walls, including a more comprehensive review of building codes, improving the simulation methods (e.g., now using 2D rather than 1D hygrothermal simulations), updating the construction materials, and including a new introduction and discussion.

This study proposes and tests a methodology that combines weather file morphing, hygrothermal simulation, and mold growth simulation to assess the risk of mold growth under expected future weather conditions. We present cases of conventional residential exterior wall assemblies that comply with current or historical building codes in three US cities and simulate their hygrothermal and mold growth performance under morphed future weather conditions.

The methodology consists of four steps.

1. The wall assembly is defined, including its layers and material properties, based on a review of applicable building codes and statistics.
2. Weather files are morphed from typical weather data to those representing future conditions using the CCWorldWeatherGen V 1.9 weather file generator (University of Southhampton, Southhampton, UK), using the IPCC Third Assessment Report climate model HadCM3 for scenario A2 [46,47].
3. The hygrothermal performance of the wall models is simulated via the modeling software WUFI 2D for the present and future climate conditions.
4. The material moisture and temperature conditions of the inner-wall cavity layer are computed to calculate the mold occurrence potential at the wood stud, using the VTT mold index model (see Section 2.6 for details) [30,48,49]. The result is a time series of mold growth indices. It was calculated hourly for five years to reach steady cyclical conditions.

2.2. The Case Cities

In earlier studies [44,45], the authors explored other US cities, including New York City, due to its large population and location within a mixed hot/humid and cold climate. This analysis focuses on the three most populous cities [22] within the ASHRAE Climate Zone 4A (CZ4A), namely New York City (NYC), Philadelphia (PA), and Washington, DC (DC), as shown in Figure 1. All three cities have comparable building codes that address historically prolonged winter conditions.

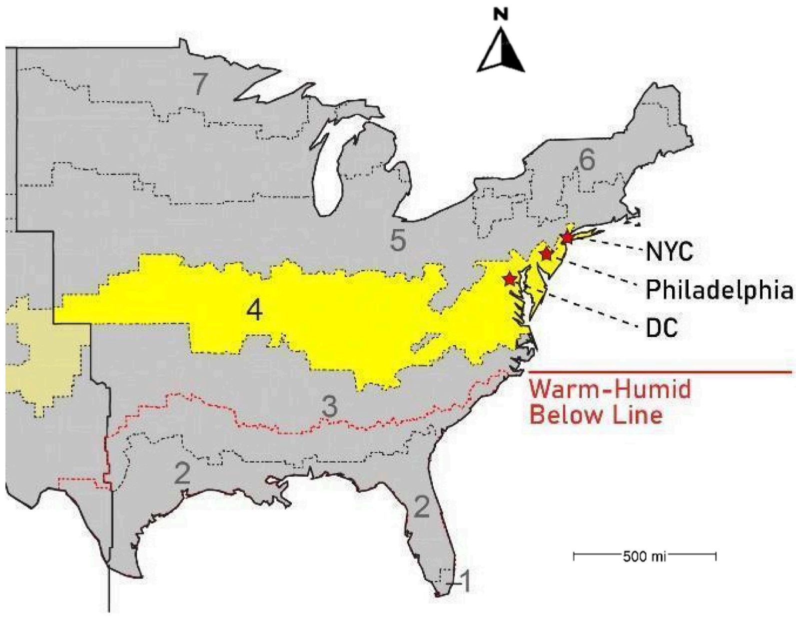

Figure 1. Three case study cities in ASHRAE Climate Zone 4A (CZ4A), shown in yellow: New York City, Philadelphia and Washington D.C. Map shows extent of CZ4A in comparison to the "warm-humid" region in the U.S. and Climate Zones 1 through 7.

2.3. Wall Assemblies and Code Compliance

Two code-compliant and conventional wall assemblies for residential buildings in these three cities were tested. All modeled wall types are lightweight wood-frame constructions due to their overwhelming popularity and the fact that wood can serve as a food source for mold. The walls are categorized by age and time of construction to illustrate the potential failure of existing walls, including one wall compliant with the building codes from the 1990s into 2000s, labeled as Wall A, and one wall type that is compliant with the current 2021 building codes, labeled as Wall B. Note that building codes vary in different locations, as states and cities adopted model codes at different times. There are different ways to design a code-compliant wall. Nevertheless, the simulated mold growth results were particularly sensitive to a single design variable: the vapor retarder's permeance. They will therefore be discussed in more detail below and in Appendices A and B.

Figure 2 shows the composition of each wall. The layers, material properties, and assembly details are based on a report by Lstiburek et al. that outlines the typical properties of construction materials in the US industry [50]. Following these specifications, the material properties in the WUFI library were altered to match, including density, thickness, and permeance of typical products available in the US.

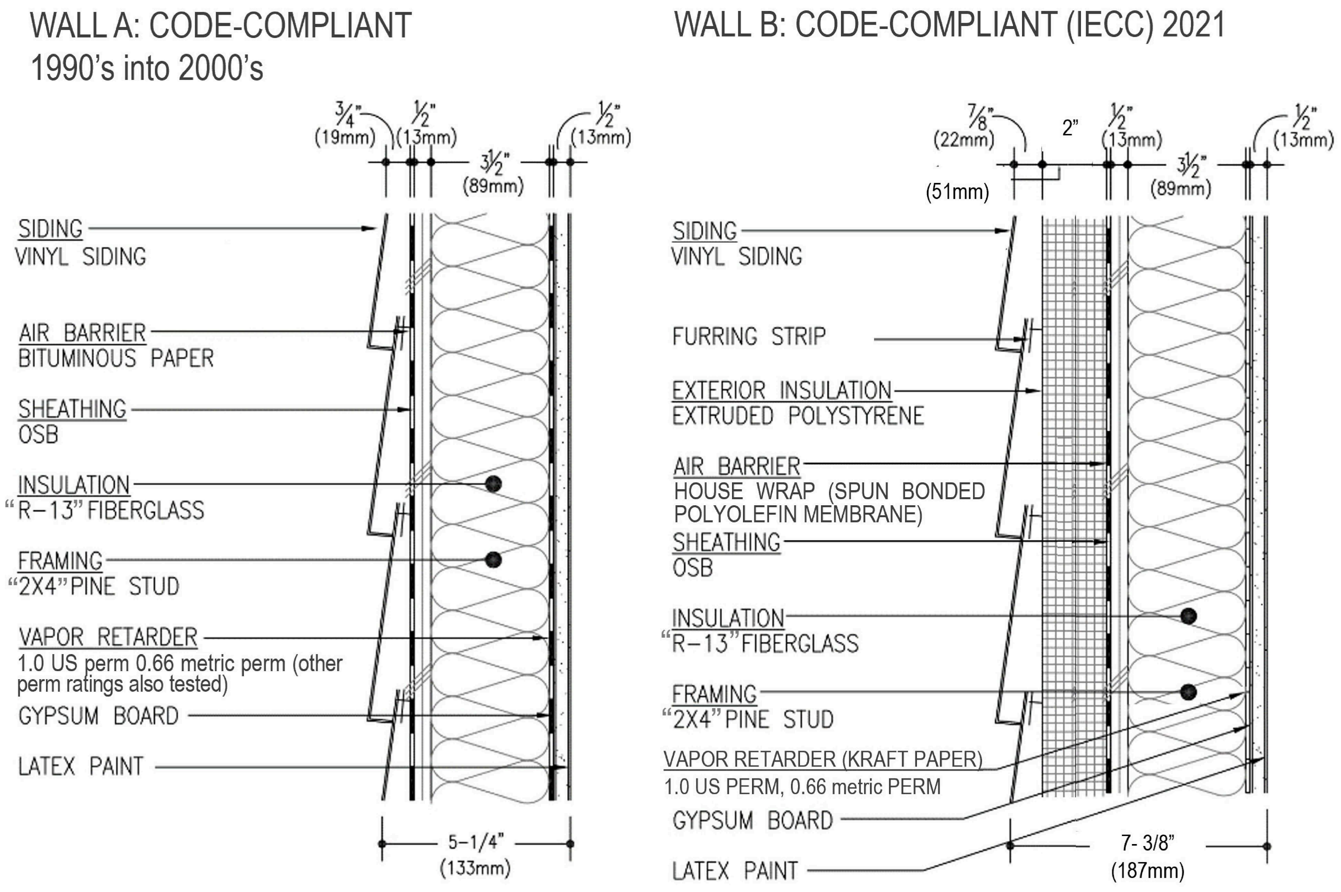

Figure 2. Two wall sections modeled in the study: Wall A, code-compliant in circa the 1990's and 2000's and Wall B, code-compliant by IECC 2021 [50–55].

Readers should be aware that the term "perm" is used in both metric and inch-pound (US) systems, and the term is not often defined, even in US literature. The US codes and building product literature are assumed to use US perms, defined as 1 grain of water vapor per hour, per square foot, per inch of mercury. Metric perms are defined as 1 gram of water vapor per day, per square meter, per millimeter of mercury. Thus, 1 metric perm is approximately 1.517 US perms.

2.3.1. Wall A

The first assembly represents a typical residential exterior wall built in the cooler US climate zones in the 1990s. The wall assembly, shown in Figure 2, consists of a series of layers enclosing a 3.8 × 9 cm (1.5 × 3.5 inch, “2 × 4”) pine stud frame. The major differences of this wall compared with current standards are a higher total U-value (with no exterior insulation) and a different air barrier. The historical wall assemblies could also include a substantially less permeable vapor-retarding membrane, so a version with a less permeable vapor retarder was tested as well. However, to be conservative, the main results presented do not include this less permeable vapor retarder.

Relatively impermeable vapor retarders were a common practice in the cooler US climate zones in the 1990s and into the 2000s. For example, the residential building codes in effect in New York City from 1991 to 2011 required a vapor retarder with a permeance of less than 1.52 metric perms (1.0 US perm) on the winter-warm side of the insulation [50,51,54,56,57]. Similar building codes were adopted across the region. For example, this vapor retarder requirement was in place in Philadelphia from circa 1997 to 2009 and in DC from 1999 to 2014 [50–53,55,58]. Eventually, codes began either to drop requirements for vapor retarders or to allow the use of more permeable materials. For example, the IECC 2018 code [59] essentially required vapor retarders with a resistance greater than 0.152 metric perms (0.1 US perm) and less than or equal to 15.2 metric perms (10 US perms) for this climate zone. For more details on the building codes of this era and their requirements, see Appendix A.

Wall A, used in the model, complies with the circa 1990s–2000s codes of the three case study cities [50–53]. See Appendix B for a breakdown of the WUFI inputs. The wall insulation is “R-13” fiberglass batt with a U-value of 0.3993 W/m^{2}K (R-13 hft^2°F/Btu), located in the stud cavity, with a vapor retarder rated at 1.52 metric perms (1.0 US perm) towards the winter-warm side of the wall, i.e., the interior. This represents a conservative case for our study because it is the most permeable vapor barrier (i.e., the presumed best case) permitted by certain historical versions of the code, as detailed in Appendix A.

As a sensitivity check, Wall A assemblies with other vapor retarders were also tested in the Washington, DC, climate. These included 0.152 metric perms (0.1 US perm) to reflect the least permeable (potentially the worst case) 1990s scenario, and 7.6 metric perms (5.0 US perms) to reflect a potentially less mold-prone case.

2.3.2. Wall B (2 × 6, R-20)

The second wall assembly is based on the 2021 IECC (International Energy Conservation Code), Chapter 4, Residential Buildings, Table R402.1.3. The chosen path is R13 cavity insulation plus R10 continuous insulation. This is relevant because in recent years, building codes in all three cities, New York City, Philadelphia, and Washington, DC, followed a trend of adopting the latest version of the IECC (see [57] and Appendix A). Here, compliance is achieved by adding 51 mm (2-inch) extruded polystyrene exterior insulation with a U-value of 0.49 W/m^{2}K. See Wall B in Figure 2.

For the vapor retarder at the interior face of the stud cavity, we simulated the interior batt insulation with a standard kraft paper facing (1.0 perm). We also replaced the air-barrier material with a more airtight spun-bonded polyolefin membrane (e.g., Tyvek, Wilmington, DE, USA), used in current construction practice as a “house-wrap” on the exterior of the sheathing to air-seal the building enclosure. For more information on wall assemblies and their simulation, see Appendix B.

https://doi.org/10.3390/buildings16132643

2.4. Weather Inputs

2.4.1. Typical Weather Conditions

We compared the performance of the defined walls under two sets of exterior conditions for each city: historical "typical" weather and morphed future weather. For typical weather, we use EnergyPlus (.epw) files with Typical Meteorological Year (TMY3) data from the US Department of Energy. These TMY3 files are an amalgamation of weather data from 1976 to 2005, drawn from the National Solar Radiation Database records for 1961–1990 and the 1991–2005 update [60]. Specifically, we used the NYC TMY3 from J.F.K. International Airport (7044860), the Philadelphia TMY3 from Philadelphia International Airport (724080), and the VA TMY3 from Arlington Ronald Reagan Washington National Airport (724050).

2.4.2. Future Weather Conditions

For future conditions, we morphed the listed TMY3 files into predicted weather for 2080 using the CCWorldWeatherGen V1.9 tool [47], which was available, open-source, and well documented at the time of the research. The method uses only the A2 projection model from the IPCC Third Assessment Report for future weather morphing [1], produced by the Hadley Center Coupled Model, version 3 (HadCM3). The A2 projection yields a 2100 CO2 concentration that falls between the more recent RCP6.0 and RCP8.5 projections from the IPCC Fifth Assessment Report [61,62]; see Figure 3. More details on climate change projections and weather assumptions are included in the Section 4. The weather generator engine superimposes "morphed" results onto existing hourly weather data series [47], producing an hourly dataset that enables detailed computation. Morphed TMY files represent statistically typical conditions rather than extreme weather events and may underestimate the peak moisture risk.

The climate file morphing method has been extended to other weather file formats, including TMY2/3, by Belcher, Hacker, and Powell (2005) [63]. While uncertainty remains, morphing weather files to estimate future conditions has been endorsed by several studies, in that the resulting localized weather files reflect climate models' predictions [47,63].

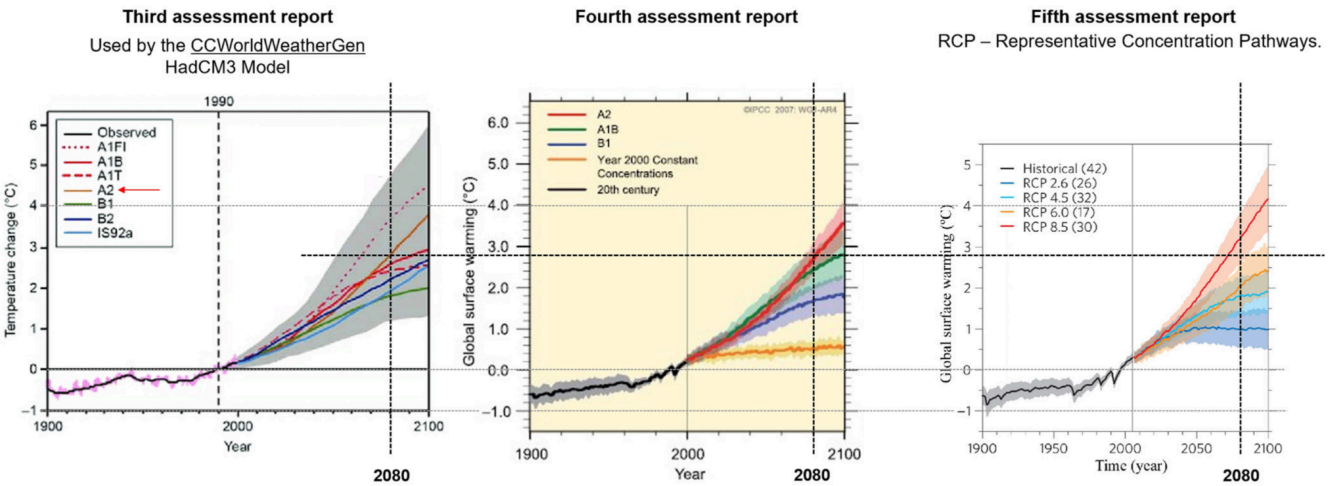

Figure 3. Comparison of the TAR A2 2080 projection [64] used in research to scenarios from the Fourth Assessment Report [62] and the Fifth Assessment Report [61]. Dashed lines show the equivalent Global Surface Warming across IPCC reports to the TAR A2 projection for 2080 used in research and available as open source via CCWorldWeatherGen.

2.4.3. Precipitation Data

Rainfall data are crucial for hygrothermal simulation due to wetting of the exterior wall's surface [44]. Unfortunately, one ongoing shortcoming of weather morphing methods for hygrothermal simulation is their inability to account for precipitation data in typical meteorological year (TMY) files, including liquid precipitation depth (mm) and liquid precipitation period (hr). Thus, the final morphed weather files do not include any precipitation data [46]. To overcome this shortcoming, we manually added the present-day rain data to the future morphed weather files. Therefore, the rain data used in our simulations do not change from present to future conditions, which is arguably a conservative approach, since, according to the Fifth IPCC assessment report, each of the studied cities (and the vast majority of the northeastern US) is projected to see more summer precipitation in all climate change scenarios [20]. This exclusion of changing precipitation patterns is a limitation, yet it shows the results under a conservative setting.

Another challenge is the methodology used to create TMY files: the selection criteria for identifying the most "typical weather" from records focused mainly on temperature, humidity, and radiation, while ignoring precipitation. This means that the rain data in a TMY file may or may not represent "typical" conditions. To test that the precipitation values used were realistic, they were compared with the WUFI Binary Climate (WBC) extreme weather files. These files represent over 30 years, the 10% coldest and the 10% warmest years, and the "ASHRAE Year 1", which is the most severe typical weather file "concerning moisture damage within the building envelopes" according to ASHRAE project RP 1325 [35]. We found that the results using our chosen weather files for each city fell between those generated by the two extreme weather files for the corresponding city. Thus, the weather files used were deemed to be acceptable here. The climate and weather models are discussed further in the Section 4.

2.5. Hygrothermal Model

This research used WUFI 2D version 3.2 [35,36], a dynamic hygrothermal software tool that simulates vapor diffusion, moisture content, and heat transport through building materials. This allows hygrothermal data to be collected from any depth within the wall and, therefore, enables an analysis of how each material experiences temperature and moisture changes over time. Input parameters are entered in three sections as follows.

1. Component, composed of the assembly of materials, compass orientation, surface transfer coefficient, and assumed initial moisture conditions;
2. Control, including the calculation period and timestep interval;
3. Climate, consisting of the hourly indoor and outdoor climate conditions.

The non-steady heat and moisture transport processes in the WUFI model are described in the following equations [65], where D_w (m^2/s) is the liquid transport coefficient, H (J/m^3) is the enthalpy of moist building material, h_v (J/kg) is the evaporation enthalpy of water, p (Pa) is the water vapor partial pressure, u (m^3/m^3) is the water content, δ (kg/msPa) is the water vapor diffusion coefficient in air, ϑ (°C) is the temperature, λ (W/mK) is the heat conductivity of moist material, μ (-) is the vapor diffusion resistance factor of dry material, ρ_w (kg/m^3) is the density of water, and φ (-) is relative humidity.

Heat transport:

$$\frac{\partial H}{\partial \vartheta}\frac{\partial \vartheta}{\partial t} = \frac{\partial}{\partial x}\left(\lambda \frac{\partial \vartheta}{\partial x}\right) + h_v \frac{\partial}{\partial x}\left(\frac{\delta}{\mu}\frac{\partial p}{\partial x}\right)$$

Moisture transport:

$$\rho_w \frac{\partial u}{\partial \varphi}\frac{\partial \varphi}{\partial t} = \frac{\partial}{\partial x}\left(\rho_w D_w \frac{\partial u}{\partial \varphi}\frac{\partial \varphi}{\partial x}\right) + \frac{\partial}{\partial x}\left(\frac{\delta}{\mu}\frac{\partial p}{\partial x}\right)$$

Full governing equations, discretization schemes, and boundary condition formulations are documented in Zirkelbach et al. [35] and the Fraunhofer IBP WUFI 2D technical manual; readers are directed to those references for complete mathematical detail [66].

Our model approximates airflow within the wall assembly using the recommended air and moisture leakage rates published in the WUFI guidelines for North American envelopes [23,66,67]. These reports for above-grade walls show calibrated settings that represent historical performance for US building assemblies. An adiabatic boundary was applied to the top and bottom of the wall assemblies, excluding the ground coupling, to model only above-grade conditions.

To minimize the impact of solar radiation, we oriented our modeled walls north to limit solar-driven drying and to establish an upper bound on mold risk, as previous literature shows that facade orientations in the shade are more likely to experience mold growth [68,69]. Our model parameters for the initial conditions and period testing followed the WUFI manual's recommendation, which states an initial condition of 80% relative humidity (RH) and 20 °C (68 °F) for frame constructions and materials exposed to open air during storage, as well as a simulation period of five years to determine whether the construction is in dynamic equilibrium and to assess changes in moisture content between years [66]. The same weather files were used for each consecutive year, thereby removing the effects of shock events and allowing seasonal patterns to be recognized.

Indoor temperatures were maintained between 21.1 °C (70 °F) and 23.9 °C (75 °F) using mechanical heating and cooling, in accordance with ASHRAE 160 [70]. Interior moisture loads (i.e., the moisture contributed to the indoor air by people and indoor activities) also followed the ASHRAE default value of 0.105 g/s. The indoor relative humidity was set to a maximum of 50% via mechanical dehumidification, a conservative WUFI setting, as a residential air-conditioning system may be unable to maintain this level of dehumidification. It is acknowledged that fixed setpoints, constant moisture generation, and maximum relative humidity conditions may not reflect real occupant behavior or system failures, yet they provide a conservative scenario of residential interior climate control. The building's volume is 500 m^3. The heating and cooling systems are controlled by a consistent setpoint deadband of 21.1 °C to 23.9 °C. As shown in the literature, in a warmer future climate, air conditioning use and annual cooling demand increase [71]. In WUFI 2D, indoor climate conditions are enforced as a boundary, and there is no option to define the cooling capacity of cooling equipment; therefore, the model assumes sufficient capacity to meet the cooling needs of the 2080 future weather to maintain an indoor climate of 23.9 °C and 50% RH. For air leakage, we used the WUFI "standard construction" with a leakage rate of 0.2 air changes per hour (ACH) between the outside and the interior of the building. For each wall assembly, we simulated the three cities. A summary of the exterior and interior boundary conditions is listed in Figure 4.

2.6. Mold Model

We used a secondary mathematical model, the mold growth model developed by VTT (Valtion Teknillinen Tutkimuskeskus) Technical Research Centre (Espoo, Finland) [48], which was empirically derived from a mold growth analysis [30]. Laboratory experimental studies with pine sapwood [49] informed the model's overlaying equations, which were later extended to include other building materials by Ojanen et al. [48]. Several research papers have validated this model, detailing the differential equations and regression models used to arrive at a mold growth index (MGI) [40,48,67]. The calculation is computed hourly. The mold growth index ranges from 0 (no mold growth) to 6 (100% coverage of mold growth), as described in Table 1. The calculation, as shown in Equation 1, allows for both mold growth and decay. The growth computation is based on three parameters: dry-bulb temperature (*T*), relative humidity (*RH*), and the construction material's sensitivity to mold growth (the coefficients k_1 and k_2). These coefficients are built into the VTT model to scale the mold equation for different building materials. Finally, *W* refers to the timber species, and *SQ* refers to the surface quality, which applies only to wood types. The SQ is calculated as 0 [30].

$$\frac{dM}{dt} = \frac{1}{7 \cdot expexp\ (-0.68lnT - 13.9lnRH + 0.14W - 0.33SQ + 66.2)} k_1 k_2 \quad (1)$$

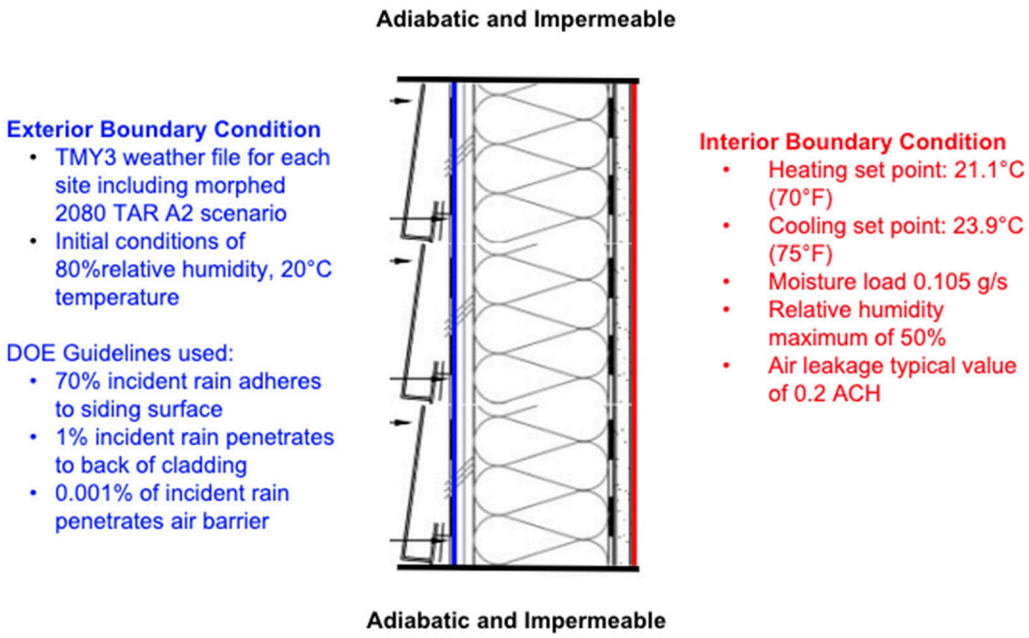

Figure 4. Boundary conditions and the initial conditions used in the WUFI model. Exterior conditions are shown in blue, interior conditions in red.

Table 1. The VTT mold growth index (MGI) [41].

Index	Growth Rate
0	No growth
1	Small amounts of mold detected only with a microscope, initial stages of local growth
2	Several local mold growth colonies on the surface detected via microscopy
3	Visual findings of mold on the surface at <10% coverage, or <50% coverage of mold (microscope)
4	Visual findings of mold on the surface, 10–50% coverage, or >50% coverage of mold (microscope)
5	Plenty of growth detected visually, >50% visual coverage
6	Very heavy and tight growth detected visually (coverage 100%)

The VTT classification of "pine sapwood" is used. It is a common material for wall studs, one of the most mold-sensitive materials in the VTT library, and is the most well-studied, as it was the base substrate studied to produce the original mathematical VTT model. The default sensitivity (k_1 and k_2) and specifications (*W* and *SQ*) of pine sapwood were used in the mold growth index simulations.

The mold growth index was calculated at multiple sensor locations at various depths within the wall stud cavity of the hygrothermal model. Hourly temperature and relative humidity data from these sensor points were exported as .csv or .asc files to assess moisture accumulation in each wall material. Relative humidity typically peaked at the interface between the vapor retarder and wall stud in Wall A, shown in Figure 5 as the blue-highlighted cells of the pine stud in the wall cavity cross-section. Therefore, we used this data as the hourly climatic environment to simulate mold growth on the surface of pine sap wood timber framing using the VTT mathematical model of mold growth.

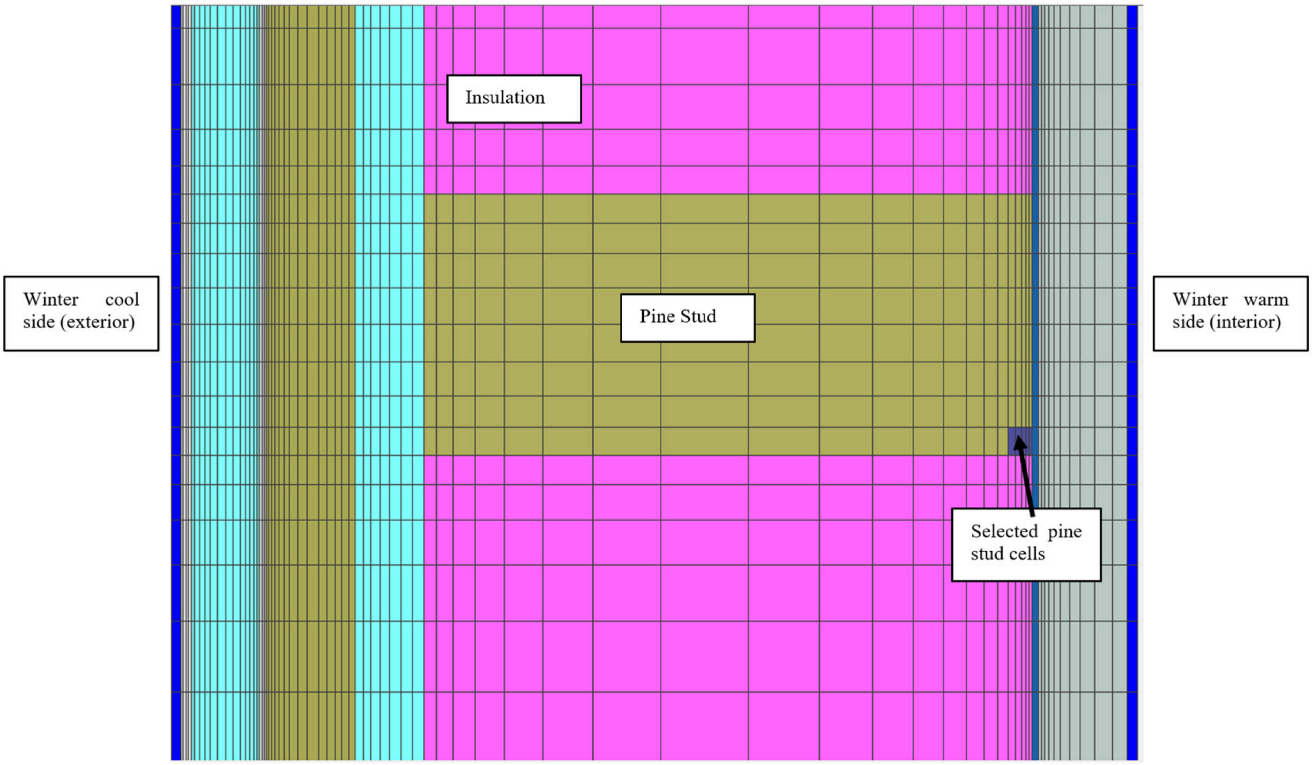

Figure 5. Horizontal cross-section of Wall A as modeled in WUFI, showing the position of the virtual sensor (indicated by the selected pine stud cells), with more details shown in Figure 2 and the Appendix B: Wall Assembly Modeling Details.

3. Results

3.1. Moisture in Walls

In all three simulated cases, future weather conditions lead to higher moisture levels within the walls. Presumably, two main factors contribute to this result. The first is the higher absolute moisture content of the outside air, and the second is the higher summertime temperature difference between a constant interior set-point temperature of 23.9 °C (75 °F) and a warmer exterior climate. Therefore, air cooled by cooler surfaces on the interior side of the wall cavity would have a higher relative humidity.

3.2. Mold Growth Results

As discussed, the simulations were run using the same year of weather data, repeated five times to account for the initial assumptions, including low moisture content and no mold. Therefore, the final year of the simulation is the most informative and is the value discussed. Here, as shown in Figure 5, the results are shown for the surface of the wood stud inside the wall cavity.

The simulated mold growth index of the modeled walls shows the stark difference in performance between present and future weather conditions. For the historical Wall A, shown in Figure 6, the present (TMY3) weather conditions resulted in microscopic mold growth that died off seasonally (mold growth index of 0). In contrast, the future (morphed) weather conditions resulted in a seasonal peak mold growth index ranging from 4 (10–50% visible mold coverage) to 5 (>50% visible mold coverage), with at least microscopic mold remaining year-round. Relative comparisons, i.e., comparing present to future or Wall A to Wall B results, are relatively robust to the mold model choice, whereas the absolute mold growth index values are not.

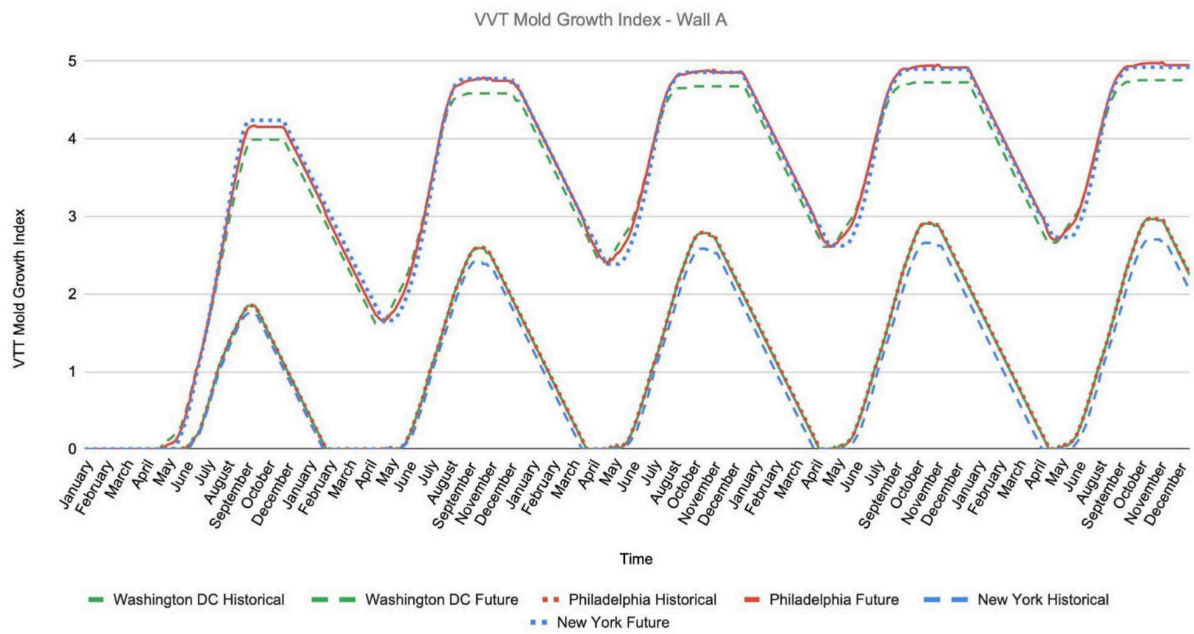

Figure 6. Simulated mold growth indices for Wall A (1.52 metric perms (1 US perm) vapor retarder) for each city, using present typical weather files (bottom) and future morphed weather files.

Fortunately, simulations of Wall B, the contemporary wall, show a mold growth index of 0 (no growth) in all walls, as shown in Figure 7. This suggests that the Wall B assembly, perhaps due to its additional exterior insulation and enhanced air barrier, improved the wall cavity temperature and relative humidity, helping prevent mold growth.

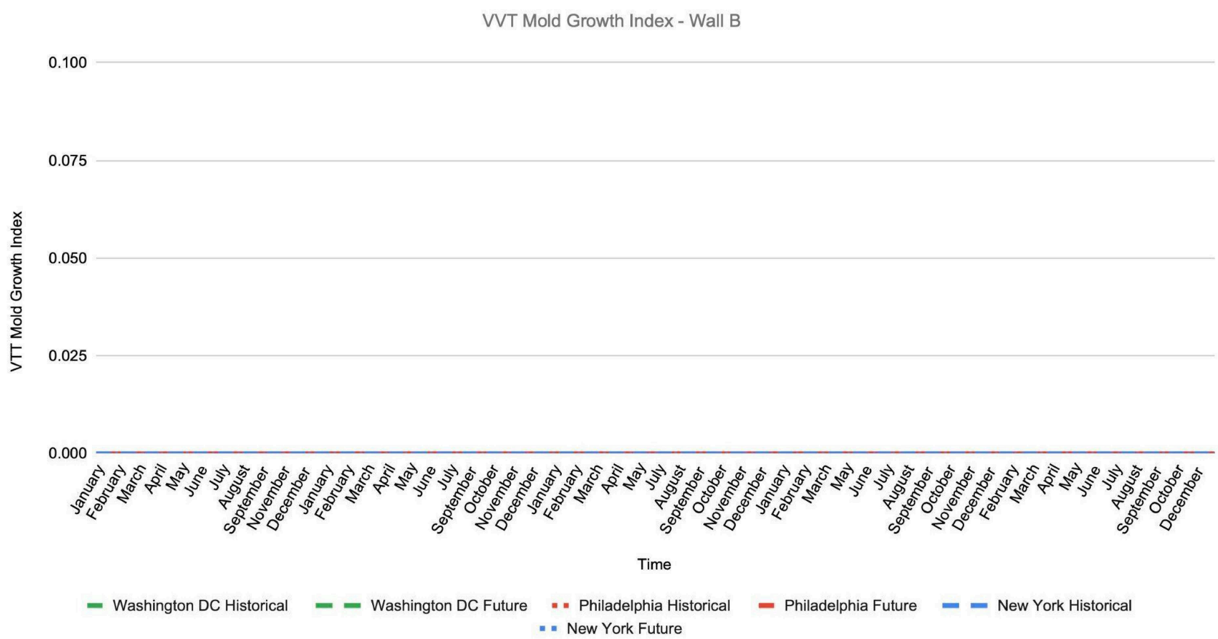

Figure 7. Simulated mold growth indices in Wall B, the more contemporary wall (again with 1.52 metric perms (1 US perm) vapor retarder) for each city, showing no simulated mold growth in all cities and weather data.

However, as with many topics in building simulation, because many model inputs are uncertain, the most important results are not the absolute predictions but the changes in the results from one test case to another. Interestingly, simulations of Wall A showed a significant increase in the simulated mold growth index from present to future weather conditions, suggesting that wall constructions susceptible to mold under today's weather may become even more susceptible under future conditions. By Year 5, the change in the mold growth index from one annual cycle to the next was minimal, indicating that additional simulation years would not yield substantive changes.

3.3. Sensitivity Checks

As explained, Wall A was tested with vapor retarders with three different permeabilities. This sensitivity check was conducted to assess future weather conditions in Washington, DC. The vapor retarder with the lowest permeability (0.152 metric perms, 0.1 US perm) resulted in the greatest mold growth, exceeding 5 on the mold growth index. This variant represents a 6 mil (0.006 inches or 0.15 mm) polyethylene membrane, a commonly used vapor retarder in historical building construction. The mid-range permeability variant is the maximum code-allowed vapor retarder, with a permeability of 1.52 metric perms (1.0 US perm), shown in Figure 6. It is associated with sustained mold growth under future climate conditions. A final 7.6-metric-perm (5.0 US perm) vapor retarder variant was tested (not compliant with the 1990s building code) and showed the lowest mold growth. Again, the important takeaway from these results is likely not the absolute estimates but their relative relationship. These results suggest that walls with less permeable vapor retarders may experience greater future mold growth.

4. Discussion

4.1. Overview of the Problem

While the health effects of mold inside walls have not been specifically studied, the general presence of mold in buildings is linked to substantial health burdens and associated costs. Research estimates annual asthma-related costs of USD 3.5 billion due to mold exposure in the home [27], while another study found that repairing mold-damaged houses and offices reduced asthma-related symptoms by 36% on average [72].

Cities in mixed US climates have optimized the construction of lightweight exterior walls for historical climates. This research simulates what will happen to these walls as the climate shifts toward a higher absolute moisture content in the outside air, hotter summers with more significant indoor/outdoor temperature differences, prolonged air-conditioning use, and warmer winters.

This research suggests that existing envelope designs may become increasingly susceptible to mold growth in future climatic conditions. Using a 2080 climate projection, the results show a significant increase in the simulated mold growth index in historical wood-frame wall assemblies, suggesting that building envelopes that are susceptible to mold growth today may become even more susceptible with climate change. This impact is a result not of climate shocks, such as flooding and storms, but of typical weather. If one were to include the impacts of such climate shocks, the threat of future mold problems would be even more severe.

4.2. Limitations

4.2.1. Future Weather Assumptions

Taking a conservative approach, our model leaves out three factors that may exacerbate future mold growth. First, as mentioned, we have used present rain data in all models. In subsequent studies, weather models should account for expected changes in precipitation (both total amounts and single events). The National Climate Assessment predicts that with a 2 °C global air temperature increase from pre-industrial levels, precipitation in the ASHRAE Climate Zone 4A could increase the 1991- 2020 baseline by 5% to 7%, and the magnitude of this change would increase to 10% to 15% under an increase of 4 °C in global air temperature [20]. On the basis of our previous research [44,45], we expect increased mold growth if future climate data incorporate these higher rainfall estimates.

Second, scholars suggest that results from weather data with morphing are likely to underestimate the effects of climate change, especially if significant mitigation action is not taken [47]. The A2 scenario from the IPCC Third Assessment Report (AR3), published in 2001, is the basis of the morphing of CCWorldWeatherGen data; it predicts a global temperature increase of +1.5 °C by 2050 and +3.8 °C by the end of the century. However, the Shared Socioeconomic Pathways (SSPs) from the IPCC Sixth Assessment Report and the Representative Concentration Pathways (RCPs) from the IPCC Fifth Assessment Report are typically used. The current business-as-usual scenario, RCP8.5, shows a global increase of over +2 °C by 2050 and an average increase of +4.6 °C by 2100 [73]. Such temperature increases would exacerbate mold growth beyond the results herein. In addition, we used a single morphed weather file for 2080 (conditions that may occur sooner, for the reasons described above) for each city, and we did not account for the warming temperatures expected after that point or in other scenarios. Therefore, these results represent a conservative prediction for mold growth for future climate scenarios.

Third, our results establish that climate stress from outdoor air temperature and humidity alone will affect the ability of the simulated walls to manage excess moisture flow. Nevertheless, further research is needed to show a complete picture of performance in a future scenario with a diversity of exterior and interior shocks, such as water leaks from storms and floods, outages, or inconsistent building operations, which could exacerbate the problem. Due to the conservative assumptions described above, the results of this study identify a seemingly distant future problem that may occur much earlier or at a higher intensity.

4.2.2. Additional Limitations/Uncertainty

The study is subject to limitations, summarized in Table 2. The general approach to the methodology, spanning data inputs and modeling decisions, was deliberately conservative. Table 2 details each limitation and its potential impact on the results.

Table 2. Additional limitations/uncertainty.

Inputs	Direction
TMY weather files show the most representative climate conditions, excluding inter-annual variability, extreme weather events, and anomalously high-humidity years.	Results are conservative.
Use of present-day precipitation data suppresses future mold risk, as climate projections indicate increased rainfall.	Results are conservative.
A single climate projection (2080) with a single emission scenario (A2, TAR) was used, as it is the only scenario available in the chosen open-source CCWordWeatherGen data.	A2, TAR, lies between the more recent RCP6.0 and RCP8.5 from the IPCC Fifth Assessment Report, representing a less severe high-emissions scenario.
Modeling	**Direction**
Only the north-facing orientation was considered.	Previous literature indicates that solar radiation inhibits mold growth [69,70]. Therefore, this research focuses on the envelope orientation expected to be most likely to support mold growth.
The model represents a typical cross-section of a wall; it does not account for higher rates of air and water leakage at corners, roof connections, and foundation lap joints.	Results are conservative, since higher air leakage in summer, and hot and humid conditions, leads to a higher risk of mold growth [74].

Table 2. *Cont.*

Mold modeling is based primarily on pine sapwood; no sensitivity analysis for other materials was conducted.	The VTT mold growth model used in the study was originally developed from laboratory tests on pine sapwood and therefore provides high-confidence results. Spruce was a later addition to the VTT material library; however, it is categorized as less sensitive and is just as common in wall construction assemblies [67]
A single mold model was used; cross-validation against other models such as the DR SIM [75] or Isaksson–Thelandersson [76] models was not performed.	The research focuses on pine sapwood because physical tests of this material form the basis of the VTT Mold Index mathematical model. Recent studies show that the VTT model underestimates mold growth for other materials, but it is highly accurate for pine sapwood [77].
Assuming steady building operation without accounting for outages, deferred maintenance, or material degradation, these conditions would increase moisture accumulation beyond the simulated values, and the results presented are conservative.	Results are conservative.
Results	Direction
Wall A and Wall B assemblies under morphed future conditions have not been validated against field measurements.	The main result is the relative change in simulated mold growth from current to expected future conditions. The absolute mold index values are not meant to be generalizable.

4.3. Implications

While it is beyond the scope of this study to determine the specific mold growth index of concern, a notable result, as shown in Figure 6, is that with climate change, the mold growth index shifts from seasonal die-off to year-round presence.

The simulations show that future weather conditions may result in a substantial increase in mold growth in light-frame wood walls, a potentially widespread future problem, due to the ubiquity of buildings with this construction type, many of which will still exist as climates shift. This study investigated three cities; however, other areas with similar climates and building practices, e.g., a substantial portion of the US in Climate Zone 4A (shown in yellow in Figure 1) and potentially elsewhere, may be similarly affected.

The chosen wall models seek to represent prevalent building practices in this region and beyond. Today, a variety of building envelope types exist, with a spectrum of susceptibility to mold growth. The main takeaway of this research is not the precise prediction of mold growth indices for a few case studies but the finding that their susceptibility to mold growth substantially increased under projected climate change.

Fortunately, in this study, the contemporary code-compliant wall model performed substantially better in preventing simulated mold growth. The contemporary wall also exhibited substantially improved energy performance for heating/cooling the building. If these mold growth simulations are accurate, avoiding mold problems could be another motivation for owners of obsolete buildings to retrofit their building envelopes.

Studies have indicated that mold remediation in buildings is very difficult and that *preventing* mold growth is a more effective strategy [78,79]. If mold damage were left unchecked to the point of requiring total demolition and replacement of the damaged wall assembly, the renovation costs could be on the order of USD 150 per square meter of wall area. A more cost-effective approach would be to address the problem proactively, for example, by bringing the wall up to the more recent code requirements (as shown as Wall B in Figure 2), which could cost on the order of USD 35 per square meter of wall area (if the existing siding were reapplied) or USD 72 per square meter if the siding were replaced. These estimates are based on RS Means cost data [80] and explained in more detail in Appendix C. Importantly, these upgrades would also substantially improve the energy efficiency of the wall assembly, highlighting a synergy between energy and hygrothermal performance upgrades.

Updating the wall to meet current code requirements (Wall B in Figure 2) addresses the risk of mold growth. This prevents moisture from becoming trapped in the wall cavity, where it can saturate at lower temperatures near the interior layers. Research shows that treating materials to be hydrophobic can also help in climate-responsive design [81]. However, we caution against using such measures, as they can further exacerbate the trapping of moisture in organic materials prone to mold growth by creating additional vapor barriers, which is counterproductive [82].

We caution readers that the methods used here are relatively new and that some model inputs are uncertain and cannot be validated. Therefore, this study should be viewed with some degree of skepticism, as it is intended as a first step in investigating the potential impact of climate change on the mold performance of historical walls in the mid-Atlantic US. However, the overall increase in simulated mold growth under future weather conditions for this common historical construction type suggests that this potentially widespread issue warrants further study.

4.4. Future Work

Empirical studies could validate the simulated findings and further underpin the existing modeling calculations, especially in three-dimensional hygrothermal studies, which are an active field of research. Future research is needed to investigate the extent of the problem, e.g., by testing different combinations of geographic locations, future climate projections, wall (and roof) assemblies, field validations, orientation parametric study, precipitation morphing, cross-validation with other mold models, extreme weather event scenario modeling, and sensitivity analyses. Research is also needed to predict the health and financial implications of such problems and to identify solutions to prevent future mold issues in new and existing buildings. These solutions could include operational (HVAC) interventions, physical retrofits to adjust the temperature profile or wall ventilation and isolation strategies to block human exposure, or other measures.

5. Conclusions

This study presents a framework for testing the mold growth potential of existing building envelopes in expected future climate conditions. It includes weather file morphing, incorporating a conservative approach to precipitation data, and hygrothermal simulation and mold growth modeling. The simulated results suggest that existing wood-framed building envelopes, including those in the mid-Atlantic region of the US (ASHRAE Climate Zone 4, Köppen Cfa, humid subtropical) built to meet the building codes of the 1990s through to the early 2000s, especially those with vapor retarders of 1.52 metric perms (1 US perm) and lower, and likely similar buildings elsewhere, will experience an increased risk of mold growth as climates change. The more modern wall section tested with exterior insulation showed no increased risk.

Northern Hemisphere builders would not construct a northern-style wall assembly in a southern climate due to differences in heat and moisture flows. However, existing constructions will increasingly be exposed to more southern-like climates. Therefore, this research sheds light on the risk of mold growth in existing building assemblies as temperatures warm, absolute humidity increases, and mechanical cooling seasons expand and intensify. The risk of mold growth from these climate stresses, rather than climate shocks, has been relatively absent from the climate resilience literature, yet the risk may be widespread, given that the wood-framed building envelopes tested here represent a large share of existing buildings, many of which are expected to remain for decades to come. Importantly, this research suggests that building assemblies adapted to historical climate conditions may be obsolete in future climates.

https://doi.org/10.3390/buildings16132643

Author Contributions: Conceptualization, H.S. and P.L.C.; methodology, H.S., P.L.C. and K.B.; formal analysis, K.B.; writing—original draft preparation, K.B. and P.L.C.; writing—review and editing, P.L.C. and H.S.; visualization, K.B. and P.L.C.; supervision, H.S.; funding acquisition, H.S. All authors have read and agreed to the published version of the manuscript.

Funding: This research was funded by the Massachusetts Institute of Technology, Harvard University Center for the Environment, a Harvard University Research Enabling Grant, and the Harvard Joint Center for Housing Studies.

Data Availability Statement: The raw data supporting the conclusions of this article will be made available by the authors on request.

Acknowledgments: We thank Sara Tepfer for her earlier simulation explorations, Kenner Carmody for help with building code research and wall section drawings, Esteban Estrella Guillén for help with code research, and Jesse Keenan of Tulane University for insights during the early conceptualization of this study. We thank Jose Gonzalez at the Philadelphia Board of Licenses and Inspections for information on the history of Philadelphia codes. During the preparation of this manuscript, the authors used Claude Haiku 4.5 and Grammarly Pro v.1.2.259.1886 to edit the original text for conciseness and grammar. The authors have reviewed and edited the output and take full responsibility for the content of this publication.

Conflicts of Interest: The funders had no role in the design of the study; In the collection, analyses, or interpretation of data; in the writing of the manuscript; or in the decision to publish the results. Furthermore, Aurora Energy Research, one of the author's current affiliation, were not involved in this study or in the preparation of the manuscript. Author Pamela Cabrera was employed by the company Transsolar Inc. The remaining authors declare that the research was conducted in the absence of any commercial or financial relationships that could be construed as a potential conflict of interest.

Appendix A. US Building Codes

Table A1 provides a history of relevant building codes and their requirements regarding vapor retarders. Table A2 indicates which code was in effect in historic years in each case city.

Table A1. History of major US building codes and vapor retarder requirements.

Code	Rules on Vapor Retarders
1990 BOCA [58]	"Vapor barriers must be considered."
1996 BOCA [53] 2000 [50], 2003 [51], 2006 [52] IECC residential	Vapor retarder *required* less than or equal to 1 perm. *
2009, 2012 IECC residential [55] 2009 IRC [83]	No mention of vapor retarder.
2009, 2015, 2018 IBC [84]	Vapor retarders *not* required for Climate Zone 4. Vapor retarders less than or equal to 0.1 perm *not* permitted for Climate Zone 4.
2015 IECC [55] 2015, 2018 IRC [83]	Vapor retarders *not* required for Climate Zone 4.
2018 [59], 2021 IECC [55]	Vapor retarder less than or equal to 0.1 perm *not* permitted. Vapor retarder greater than 0.1 and less than or equal to 10 perms *required.*

* 1 perm = 5.7×10^{-11} kg/(Pa s m^2).

Table A2. History of building codes and vapor retarders' requirements for New York City, Philadelphia, and Washington, DC.

Year [1]	Official Code (or Model Code Used as the Basis of the Local Code)	Rules on Vapor Retarders
	New York City	
1991	NY State ECC 1991 [54]	Vapor retarder *required* less than or equal to 1 perm. *
2002	IECC 2000 [50]	
2008	IECC 2003 [51]	
2011	NY City ECC 2011 [57]	Vapor retarders *not* required for Climate Zone 4.
2016	NY City ECC 2016 [57]	No mention of vapor retarder.
2020	IECC 2018 [55]	Vapor retarder less than or equal to 0.1 perm *not* permitted. Vapor retarder greater than 0.1 and less than or equal to 10 perms *required.*
	Philadelphia	
The early 1990s assumed	BOCA 1990 [58]	"Vapor barriers must be considered."
Late 1990s assumed	BOCA 1996 [53]	Vapor retarder *required* less than or equal to 1 perm.*
2004	IECC 2003 [51]	
2006	IECC 2006 [52]	
2009	IECC 2009 [55]	No mention of vapor retarder.
2015	IECC 2015 [55]	Vapor retarders not required for Climate Zone 4.
2022	IECC 2018 [55]	Vapor retarder less than or equal to 0.1 perm *not* permitted. Vapor retarder greater than 0.1 and less than or equal to 10 perms *required.*
	Washington DC	
1992	BOCA 1990 [58]	"Vapor barriers must be considered."
1999	BOCA 1996 [53]	Vapor retarder *required* less than or equal to 1 perm. *
2004	IECC 2000 [50]	
2008	IECC 2006 [52]	
2014	IECC 2012 [55]	No mention of vapor retarder.
2020	IECC 2015 [55]	Vapor retarders *not* required for Climate Zone 4.

* 1 perm = 5.7×10^{-11} kg/(Pa s m^2). [1] The history of building code adoption was accessed from the US Department of Energy Building Codes Program website (https://www.energycodes.gov/state-portal; last accessed 10 May 2024). Earlier, Philadelphia's code adoption was based on an interview with Jose Gonzalez at the Board of Licenses and Inspections Review in the City of Philadelphia.

Appendix B. Wall Assembly Modeling Details

Appendix B.1. Methods, Wall Assemblies, and Code Compliance/Models

- The wall labels refer to typical US naming conventions based on nominal stud sizes, 14 "2 × 4" or "2 × 6" (actually 1.5 × 3.5 or 1.5 × 5.5 inches), and insulation R-values (in ft2 °F/Btu).
- Revised density properties in our model: oriented strand board, 576.6 kg/m^3 (36 pounds/ft3); low-density fiberglass insulation, 19.2 kg/m^3 (1.2 pounds/ft3); and higher-density gypsum board, 800.9 kg/m3 (50 pounds/ft3) [23].
- Lightweight timber framing is the most ubiquitous construction type for North American housing, and vinyl siding represents the most ubiquitous envelope material used in housing on the Northeast coast of the US. About 73% of the homes built before 2000 in the Middle Atlantic census division, which includes Philadelphia and NYC, have vinyl siding, and about 40% of homes in the South Atlantic census division,

which includes Washington, DC, use vinyl siding. Vinyl remains the leading material for residential siding [22].

Appendix B.2. Methods: Hygrothermal Model

- DOE guidelines used for our models include the following: 70% incident rain adheres to the siding surface and is addressed by liquid conductivity and vapor diffusion, and the remaining 30% sheds off the surface; 1% of incident rain to the siding penetrates to the back of the cladding, and 0.01% of the incident rain penetrates the air barrier and reaches the sheathing. The flow rates to the interior layers of the wall depend on the siding material: for vinyl siding, we model a flow rate of 0.5 cfm/sf, an air change per hour (ACH) of 200, and gaps of 3/16″ for the cladding ventilation, plus 10 ACH for sheathing the exterior and interior ventilation. For painted wood siding (southern yellow pine), the gap size and flow rate on either side of the sheathing remain the same, but the flow rate decreases to 0.1 cfm/sf and 20 ACH for cladding ventilation. [23].
- For reference, Passive House standards require a maximum of 0.6 ACH at 50 Pascals of pressure, which would equate to approximately 0.03 ACH or less under natural conditions.
- Figures A1 and A2 provides additional details on the simulation settings of Wall A and Wall B, repectively.

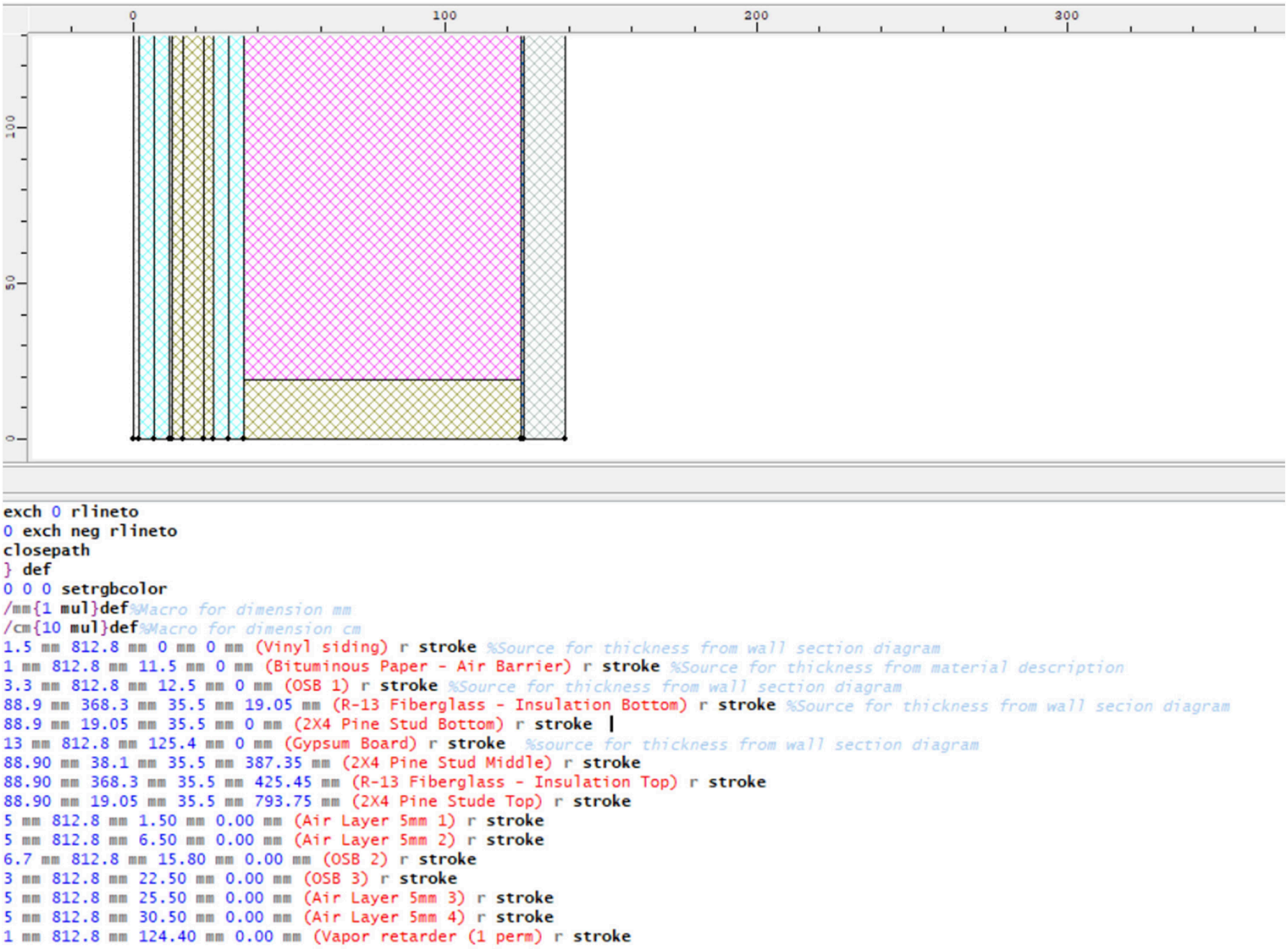

Figure A1. Wall A's simulation settings. Dark blue text indicates layer thickness, red text indicates material description, light blue text indicates the source of the input, and black text is other WUFI simulation text. The colored hatching distinguishes the material layers from each other.

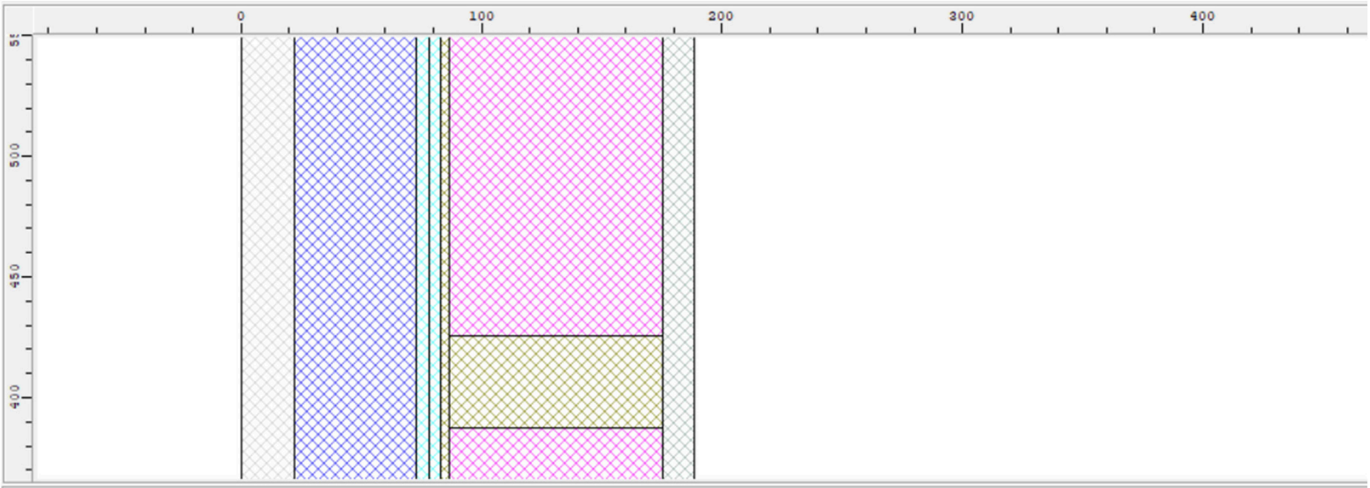


```
/r{%Macro for rectangle. Parameter: width height left bottom
newpath
name
moveto
dup 0 exch rlineto
exch 0 rlineto
0 exch neg rlineto
closepath
} def
0 0 0 setrgbcolor
/mm{1 mul}def%Macro for dimension mm
/cm{10 mul}def%Macro for dimension cm
22 mm 812.8 mm 0 mm 0 mm (Vinyl siding) r stroke %Source for thickness from wall section diagram
51 mm 812.8 mm 22 mm 0 mm (extruded polystyrene 1 R-10)  r stroke
5 mm 812.8 mm 73 mm 0 mm (air layer 5mm 1)  r stroke
5 mm 812.8 mm 78 mm 0 mm (air layer 5mm) r stroke
3.3 mm 812.8 mm 83 mm 0 mm (OSB 1) r stroke %Source for thickness from wall section diagram
89 mm 368.3 mm 86.3 mm 19.05 mm (R-13 Fiberglass - Insulation Bottom) r stroke %Source for thickness from wall secion diagram
89 mm 19.05 mm 86.3 mm 0 mm (2X4 Pine Stud Bottom) r stroke |
89 mm 38.1 mm 86.3 mm 387.35 mm (2X4 Pine Stud Middle) r stroke
89 mm 368.3 mm 86.3 mm 425.45 mm (R-13 Fiberglass - Insulation Top) r stroke
89 mm 19.05 mm 86.3 mm 793.75 mm (2X4 Pine Stude Top) r stroke
13 mm 812.8 mm 175.3 mm 0 mm (Gypsum Board) r stroke  %source for thickness from wall section diagram
```

Figure A2. Wall B's simulation settings. Dark blue text indicates layer thickness, red text indicates material description, light blue text indicates the source of the input, and black text is other WUFI simulation text. The colored hatching distinguishes the material layers from each other.

Appendix C. Remediation Cost Estimates

These estimates, using the RS Means database [80], are based on US average costs, including materials and labor, but exclude demolition and disposal costs.

Appendix C.1. Total Replacement of Mold-Degraded Materials

This estimate includes new "2 × 4" wood studs, plywood sheathing, fiberglass batt, and drywall, totaling USD 150 per square meter of wall assembly (USD 14 per square foot).

Appendix C.2. Addition of New Air Barrier and Insulation Only

This estimate includes a new air barrier and 51 mm (2 inches) of extruded polystyrene insulation, totaling USD 35 per square meter of wall assembly (USD 3.20 per square foot).

Appendix C.3. Addition of New Air Barrier and Insulation, with Siding Replacement

This estimate includes the insulation and air barrier listed above, plus replacement vinyl siding, for a total of USD 72 per square meter of wall assembly (USD 6.70 per square foot).

As an alternative, the siding could be replaced with cedar clapboard cladding rather than vinyl siding, at a total cost of USD 104 per square meter of wall assembly (USD 9.65 per square foot).

References

1. McCarthy, J.J.; Canziani, O.F.; Leary, N.A.; Dokken, D.J.; White, K.S. *Climate Change 2001: Impacts, Adaptation, and Vulnerability: Contribution of Working Group II to the Third Assessment Report of the Intergovernmental Panel on Climate Change*; Cambridge University Press: Cambridge, UK, 2001; Volume 2.
2. Wan, K.K.; Li, D.H.; Pan, W.; Lam, J.C. Impact of climate change on building energy use in different climate zones and mitigation and adaptation implications. *Appl. Energy* **2012**, *97*, 274–282. [CrossRef]
3. Huang, K.T.; Hwang, R.L. Future trends of residential building cooling energy and passive adaptation measures to counteract climate change: The case of Taiwan. *Appl. Energy* **2016**, *184*, 1230–1240. [CrossRef]
4. Almås, A.J.; Lisø, K.R.; Hygen, H.O.; Øyen, C.F.; Thue, J.V. An approach to impact assessments of buildings in a changing climate. *Build. Res. Inf.* **2011**, *39*, 227–238. [CrossRef]
5. De Wilde, P.; Coley, D. The implications of a changing climate for buildings. *Build. Environ.* **2012**, *55*, 1–7. [CrossRef]
6. Schroderus, S.; Lähteenmäki, V.M.; Barbero-López, A.; Haapala, A.; Fedorik, F. Effect of climate change on hygrothermal performance of timber framed wall with different insulation materials. *Build. Environ.* **2025**, *269*, 112438.
7. Wang, L.; Ge, H. Effect of rain leakage on hygrothermal performance of highly insulated wood-framed walls: A stochastic approach. *Can. J. Civ. Eng.* **2019**, *46*, 979–989. [CrossRef]
8. Aggarwal, C.; Ge, H.; Defo, M. Assessing mould growth risk of wood-frame walls using partial least squares (PLS) regression considering climate model uncertainties. *Build. Environ.* **2023**, *238*, 110374. [CrossRef]
9. Nik, V.M.; Mundt-Petersen, S.O.; Kalagasidis, A.S.; De Wilde, P. Future moisture loads for building facades in Sweden: Climate change and wind-driven rain. *Build. Environ.* **2015**, *93*, 362–375. [CrossRef]
10. Nik, V.M.; Kalagasidis, A.S.; Kjellström, E. Assessment of hygrothermal performance and mould growth risk in ventilated attics in respect to possible climate changes in Sweden. *Build. Environ.* **2012**, *55*, 96–109. [CrossRef]
11. Defo, M.; Wang, L.; Lacasse, M.A.; Moore, T.V. Evaluation of Moisture Performance of Tall Wood Building Envelope under Climate Change in Different Canadian Climatic Regions. *Forests* **2023**, *14*, 718. [CrossRef]
12. Piggot-Navarrete, J.; Blanchet, P.; Cabral, M.R.; Perez, C. Investigating the impact of construction workmanship defects on the hygrothermal performance and airtightness of lightweight-structure wooden envelope systems. *Build. Environ.* **2023**, *243*, 110705. [CrossRef]
13. Paneru, D.; Croyle, B.; Wimmers, G.; Gaur, A.; Mukhopadhyaya, P. Impact of climate change on hygrothermal durability of exterior, non-load-bearing mass timber wall. *J. Build. Eng.* **2025**, *106*, 112558.
14. Stackhouse, P.W., Jr.; Chandler, W.S.; Hoell, J.M.; Westberg, D.; Zhang, T. *An Assessment of Actual and Potential Building Climate Zone Change and Variability from the Last 30 Years Through 2100 Using NASA's MERRA and CMIP5 Simulations*; NASA Langley Research Center: Hampton, VA, USA, 2015.
15. US Government Accountability Office (GAO). *Improved Federal Coordination Could Facilitate Use of Forward-Looking Climate Information in Design Standards, Building Codes, and Certifications*; GAO Publication No. 17-3; US Government Printing Office: Washington, DC, USA, 2016.
16. Averill, J.D.; McAllister, T.; Persily, A.K.; Weaver, S.; Whetstone, J.; Ruiz-Barradas, A. *Workshop on Incorporating Climate Change Data in US Building Codes and Standards*; US Department of Commerce: Washington, DC, USA; National Institute of Standards and Technology: Gaithersburg, MD, USA, 2023.
17. Kurth, M.; Keenan, J.M.; Sasani, M.; Linkov, I. Defining Resilience for the Building Industry for the U.S. *Build. Res. Inf.* **2018**, *47*, 480–492.
18. Langmans, J.; Klein, R.; Roels, S. Hygrothermal risks of using exterior air barrier systems for highly insulated light weight walls: A lab. investigation. *Build. Environ.* **2012**, *56*, 192–202.
19. American Society of Heating, Refrigerating and Air-Conditioning Engineers. *ASHRAE Standards: ANSI/ASHRAE Standard 169 Climatic Data For Building Design Standards*; ASHRAE: Atlanta, GA, USA, 2020.
20. Crimmins, A.R.; Avery, C.W.; Easterling, D.R.; Kunkel, K.E.; Stewart, B.C.; Maycock, T.K. (Eds.) *U.S. Global Change Research Program (USGCRP), Fifth National Climate Assessment*; U.S. Global Change Research Program: Washington, DC, USA, 2023.
21. Brown, P.J.; DeGaetano, A.T. Trends in US surface humidity, 1930–2010. *J. Appl. Meteorol. Climatol.* **2013**, *52*, 147–163. [CrossRef]
22. U.S. Census Bureau Survey of Construction (SOC). American Community Survey, 2010 New Residential Construction. Available online: https://www.census.gov/construction/chars/ (accessed on 27 November 2019).
23. Lstiburek, J.; Ueno, K.; Musunuru, S. *Strategy Guideline: Modeling Enclosure Design in Above-Grade Walls*; No. NREL/SR-5500-65479; DOE/GO-102016-4837; National Renewable Energy Laboratory (NREL): Golden, CO, USA, 2016.

24. Brasche, S.; Bischof, W. Daily time spent indoors in German homes–baseline data for the assessment of indoor exposure of German occupants. *Int. J. Hyg. Environ. Health* **2005**, *208*, 247–253. [CrossRef] [PubMed]
25. Klepeis, N.E.; Nelson, W.C.; Ott, W.R.; Robinson, J.P.; Tsang, A.M.; Switzer, P.; Behar, J.V.; Hern, S.C.; Engelmann, W.H. The National Human Activity Pattern Survey (NHAPS): A resource for assessing exposure to environmental pollutants. *J. Expo. Sci. Environ. Epidemiol.* **2001**, *11*, 231. [CrossRef]
26. Heseltine, E.; Rosen, J. (Eds.) *WHO Guidelines for Indoor Air Quality: Dampness and Mould*; WHO Regional Office Europe: Copenhagen, Denmark, 2009.
27. Mudarri, D.; Fisk, W.J. Public health and economic impact of dampness and mold. *Indoor Air* **2007**, *17*, 226–235. [CrossRef] [PubMed]
28. Tietze, A.; Ott, S.; Boulet, S.; Gradeci, K.; Labonnote, N.; Grynning, S.; Noreen, J.; Pousette, A. *Tall Timber Facades—Identification of Cost-Effective and Resilient Envelopes for Wood Constructions Scientific Project Report*; Technical University Munich: Munich, Germany, 2017.
29. Arumala, J.O. Mold and the construction industry. *Int. J. Constr. Educ. Res.* **2006**, *2*, 75–89. [CrossRef]
30. Hukka, A.; Viitanen, H.A. A mathematical model of mould growth on wooden material. *Wood Sci. Technol.* **1999**, *33*, 475–485. [CrossRef]
31. Viitanen, H.A. Modeling the time factor in the development of mould fungi-The effect of critical humidity and temperature conditions on pine and spruce sapwood. *Holzforsch. Int. J. Biol. Chem. Phys. Technol. Wood* **1997**, *51*, 6–14.
32. Pihelo, P.; Kikkas, H.; Kalamees, T. Hygrothermal performance of highly insulated timber-frame external wall. *Energy Procedia* **2016**, *96*, 685–695. [CrossRef]
33. Hall, M.R.; Casey, S.P.; Loveday, D.L.; Gillott, M. Analysis of UK domestic building retrofit scenarios based on the E. ON Retrofit Research House using energetic hygrothermics simulation–Energy efficiency, indoor air quality, occupant comfort, and mould growth potential. *Build. Environ.* **2013**, *70*, 48–59.
34. Schroderus, S.; Kuurola, P.; Kempe, M.; Fedorik, F.; Leivo, V.; Haverinen-Shaughnessy, U. Impacts of building energy retrofits on energy consumption, indoor environment, and hygrothermal performance in future climate scenarios. *Energy Build.* **2025**, *347*, 116413. [CrossRef]
35. Zirkelbach, D.; Schmidt, T.; Kehrer, M.; Künzel, H.M. *Wufi® Pro–Manual*; Fraunhofer Institute: Stuttgart, Germany, 2007.
36. Fraunhofer Institute. *Wufi® 2D Installation & Introduction*; Fraunhofer Institute: Stuttgart, Germany, 2024.
37. Fedorik, F.; Illikainen, K. HAM and mould growth analysis of a wooden wall. *Int. J. Sustain. Built Environ.* **2013**, *2*, 19–26. [CrossRef]
38. Kalamees, T.; Vinha, J. Hygrothermal calculations and laboratory tests on timber-framed wall structures. *Build. Environ.* **2003**, *38*, 689–697. [CrossRef]
39. Gradeci, K.; Labonnote, N.; Time, B.; Köhler, J. A probabilistic-based methodology for predicting mould growth in façade constructions. *Build. Environ.* **2018**, *128*, 33–45. [CrossRef]
40. Gradeci, K.; Labonnote, N.; Köhler, J.; Time, B. Mould models applicable to wood-based materials–a generic framework. *Energy Procedia* **2017**, *132*, 177–182. [CrossRef]
41. Janssens, K.; Vandemeulebroucke, I.; Marincioni, V.; Van Den Bossche, N. Hygrothermal risk assessment tool for brick walls in a changing climate. *J. Build. Phys.* **2024**, *48*, 420–441. [CrossRef]
42. Coelho, G.B.A.; Kraniotis, D. Numerical investigation of mould growth risk in a timber-based facade system under current and future climate scenarios. *J. Phys. Conf. Ser.* **2023**, *2654*, 012019. [CrossRef]
43. Conroy, A.; Mukhopadhyaya, P.; Wimmers, G. Hygrothermal response of a wood-frame thick-wall assembly to rainwater wetting under future climate scenarios in Canada. *J. Build. Phys.* **2024**, *47*, 557–579.
44. Cabrera, P.; Samuelson, H.; Kurth, M. Simulating Mold Risks Under Future Climate Conditions. In Proceedings of the 16th IBPSA Conference, Rome, Italy, 2–4 September 2019.
45. Tepfer, S.; Samuelson, H. Hygrothermal and Mold Modeling of Building Envelopes under Future Climate Conditions. In *Planning Post Carbon Cities: 35th PLEA Conference on Passive and Low Energy Architecture, A Coruña, 1st–3rd September 2020: Proceedings*; Universidade da Coruña: Coruña, Spain, 2020.
46. Jentsch, M.F. *Climate Change Weather File Generators*; Technical Reference Manual for the CCWeatherGen and CCWorldWeatherGen Tools; University of Southampton: Southampton, UK, 2010.
47. Jentsch, M.F.; James, P.A.; Bourikas, L.; Bahaj, A.S. Transforming existing weather data for worldwide locations to enable energy and building performance simulation under future climates. *Renew. Energy* **2013**, *55*, 514–524. [CrossRef]
48. Ojanen, T.; Viitanen, H.; Peuhkuri, R.; Lähdesmäki, K.; Vinha, J.; Salminen, K. Mold-growth modeling of building structures using sensitivity classes of materials. In Proceedings of the Buildings XI, Clearwater Beach, FL, USA, 5–9 December 2010.
49. Viitanen, H.; Ritschkoff, A.C. *Mould Growth in Pine and Spruce Sapwood in Relation to Air Humidity and Temperature*; Institutionen för Virkeslära: Uppsala, Sweden, 1991.

50. International Code Council. 2000 International Energy Conservation Code. 2000. Available online: https://codes.iccsafe.org/content/IECC2000 (accessed on 19 June 2026).
51. International Code Council. 2003 International Energy Conservation Code. 2003. Available online: https://codes.iccsafe.org/content/IECC2003 (accessed on 19 June 2026).
52. International Code Council. 2006 International Energy Conservation Code. 2006. Available online: https://codes.iccsafe.org/content/IECC2006 (accessed on 19 June 2026).
53. Building Officials and Code Administrators. *The BOCA National Energy Conservation Code 1996*; Building Officials & Code Administrators International, Inc.: Country Club Hills, IL, USA, 1996.
54. NY State ECC, New York State Department of State. *New York State Energy Conservation Construction Code*; New York State Department of State: Albany, NY, USA, 1991.
55. International Code Council. International Energy Conservation Code. 2009, 2012, 2015, 2018, 2021. Available online: https://codes.iccsafe.org/ (accessed on 19 June 2026).
56. New York State Department of State. New York State Energy Conservation Construction Code, Part 3, Section 7813.3 Thermal Performance of Envelope Systems. Available online: https://www.dos.ny.gov/dcea/pdf/nyseccc.pdf (accessed on 10 May 2024).
57. NY City ECC. *New York City Energy Conservation Code*; New York City Department of Buildings: New York, NY, USA, 2016.
58. Building Officials and Code Administrators. *The BOCA National Energy Conservation Code 1990*, 6th ed.; Building Officials & Code Administrators International, Inc.: Country Club Hills, IL, USA, 1990.
59. International Code Council. 2018 International Energy Conservation Code. 2018. Available online: https://codes.iccsafe.org/content/IECC2018 (accessed on 10 May 2024).
60. Wilcox, S.; Marion, W. *User's Manual for TMY3 Data Sets*; National Renewable Energy Laboratory: Golden, CO, USA, 2008.
61. Intergovernmental Panel on Climate Change (IPCC). *Working Group 1, Summary for Policymakers. Contribution of Working Group I to the Fifth Assessment Report of the Intergovernmental Panel on Climate Change, 3, 159–204*; IPCC: Geneva, Switzerland, 2013.
62. Intergovernmental Panel on Climate Change (IPCC). *Climate Change 2007: The Physical Science Basis. Contribution of Working Group I to the Fourth Assessment Report of the Intergovernmental Panel on Climate Change*; Solomon, S., Qin, D., Manning, M., Chen, Z., Marquis, M., Averyt, K.B., Tignor, M., Miller, H.L., Eds.; Cambridge University Press: Cambridge, UK; New York, NY, USA, 2007.
63. Belcher, S.E.; Hacker, J.N.; Powell, D.S. Constructing design weather data for future climates. *Build. Serv. Eng. Res. Technol.* **2005**, *26*, 49–61. [CrossRef]
64. IPCC. Summary for policymakers. In *Climate Change 2001: The Scientific Basis. Contribution of Working Group I to the Third Assessment Report of the Intergovernmental Panel on Climate Change*; Houghton, J.T., Ding, Y., Griggs, D.J., Noguer, M., van der Linden, P.J., Dai, X., Maskell, K., Johnson, C.A., Eds.; Cambridge University Press: Cambridge, UK, 2001; pp. 1–20.
65. Details: Physics—Wufiwiki. Wufi-wiki.com. 8 July 2009. Available online: https://www.wufi-wiki.com/mediawiki/index.php/Details:Physics (accessed on 19 June 2026).
66. Fraunhofer Institute for Building Physics IBP. *WUFI® Pro 6 Manual*; Fraunhofer IBP: Stuttgart, Germany, 2019. Available online: https://wufi.de/en/wp-content/uploads/sites/11/WUFIPro_6_manual.pdf (accessed on 10 June 2026).
67. Viitanen, H.; Krus, M.; Ojanen, T.; Eitner, V.; Zirkelbach, D. Mold risk classification based on comparative evaluation of two established growth models. *Energy Procedia* **2015**, *78*, 1425–1430. [CrossRef]
68. Guan, L.; Dewsbury, M.; Wallis, L.; Kuenzel, H. Navigating Energy Efficiency and Mould Risk in Australian Low-Rise Homes: A Comparative Analysis of Nine External Wall Systems in Southeast Australia. *Energies* **2025**, *18*, 2843. [CrossRef]
69. Gasparri, E.; Brambilla, A.; Aitchison, M. Hygrothermal analysis of timber-based external walls across different Australian climate zones. In Proceedings of the WCTE 2018, World Conference on Timber Engineering, Seoul, Republic of Korea, 20–23 August 2018.
70. TenWolde, A. *ASHRAE Standard 160P--Criteria for Moisture Control Design Analysis in Buildings*; ASHRAE: Atlanta, GA, USA, 2008.
71. Amonkar, Y.; Doss-Gollin, J.; Farnham, D.J.; Modi, V.; Lall, U. Differential effects of climate change on average and peak demand for heating and cooling across the contiguous USA. *Commun. Earth Environ.* **2023**, *4*, 402. [CrossRef]
72. Sauni, R.; Uitti, J.; Jauhiainen, M.; Kreiss, K.; Sigsgaard, T.; Verbeek, J.H. Remediating buildings damaged by dampness and mould for preventing or reducing respiratory tract symptoms, infections and asthma (Review). *Evid. Based Child Health* **2013**, *8*, 944–1000. [CrossRef] [PubMed]
73. IPCC. *Climate Change 2014: Impacts, Adaptation, and Vulnerability. Summaries, Frequently Asked Questions, and Cross-Chapter Boxes. A Contribution of Working Group II to the Fifth Assessment Report of the Intergovernmental Panel on Climate Change*; Field, C.B., Barros, V.R., Dokken, D.J., Mach, K.J., Mastrandrea, M.D., Bilir, T.E., Chatterjee, M., Ebi, K.L., Estrada, Y.O., Genova, R.C., et al., Eds.; World Meteorological Organization: Geneva, Switzerland, 2014.
74. Li, Y.; Dang, X.; Xia, C.; Ma, Y.; Ogura, D.; Hokoi, S. The effect of air leakage through the air cavities of building walls on mold growth risks. *Energies* **2020**, *13*, 1177. [CrossRef]
75. Boardman, C.R.; Glass, S.V.; Lepage, R. Dose-response simple isopleth for mold (DR SIM): A dynamic mold growth model for moisture risk assessment. *J. Build. Eng.* **2023**, *68*, 106092. [CrossRef]

76. Isaksson, T.; Brischke, C.; Thelandersson, S. Development of decay performance models for outdoor timber structures. *Mater. Struct.* **2013**, *46*, 1209–1225.
77. Glass, S.V.; Lepage, R.; Farkas, N.; Zelinka, S.L. Comparative Evaluation of the VTT Mold Index Model and the DR SIM Model for Moisture Risk Assessment. In *Paper in Proceedings*; Forest Products Laboratory: Madison, WI, USA, 2025.
78. Peitzsch, M.; Bloom, E.; Haase, R.; Must, A.; Larsson, L. Remediation of mould damaged building materials—Efficiency of a broad spectrum of treatments. *J. Environ. Monit.* **2012**, *14*, 908–915. [CrossRef] [PubMed]
79. Haverinen-Shaughnessy, U.; Hyvärinen, A.; Putus, T.; Nevalainen, A. Monitoring success of remediation: Seven case studies of moisture and mold damaged buildings. *Sci. Total Environ.* **2008**, *399*, 19–27. [CrossRef] [PubMed]
80. The Gordian Group. RSMeans Data Online. Available online: https://www.rsmeansonline.com/ (accessed on 17 June 2026).
81. Ortega Del Rosario, M.D.L.Á.; Beermann, K.; Chen Austin, M. Environmentally responsive materials for building envelopes: A review on manufacturing and biomimicry-based approaches. *Biomimetics* **2023**, *8*, 52. [CrossRef] [PubMed]
82. Al-Shatnawi, Z.; Hachem-Vermette, C.; Lacasse, M.; Ziaeemehr, B. Advances in cold-climate-responsive building envelope design: A comprehensive review. *Buildings* **2024**, *14*, 3486.
83. International Code Council. IRC: International Residential Code for One- and Two-Family Dwellings (IRC-2009, 2015, 2018 eds.). 2009, 2015, 2018. Available online: https://codes.iccsafe.org/ (accessed on 10 June 2026).
84. International Code Council. IBC: International Building Code (2009, 2015, 2018 eds.). 2009, 2015, 2018. Available online: https://codes.iccsafe.org/ (accessed on 10 June 2026).

https://doi.org/10.3390/buildings16132643